IEEE Access
Multidisciplinary | Rapid Review | Open Access Journal

Received September 5, 2019, accepted October 27, 2019, date of publication October 30, 2019, date of current version November 14, 2019.

Digital Object Identifier 10.1109/ACCESS.2019.2950366

Identity Authentication Using Portable Electroencephalography Signals in Resting States

RONGKAI ZHANG[1], BIN YAN[1], LI TONG[1], JUN SHU[1], XIAOXIAO SONG[1,2], AND YING ZENG[1,3]

[1]Department of Information System Engineering, PLA Strategy Support Force Information Engineering University, Zhengzhou 450001, China
[2]Henan Information Center, Zhengzhou 450003, China
[3]The Clinical Hospital of Chengdu Brain Science Institute, MOE Key Laboratory for Neuroinformation, University of Electronic Science and Technology of China, Chengdu 610000, China

Corresponding author: Ying Zeng (yingzeng@uestc.edu.cn)

This work was supported in part by the National Key Research and Development Plan of China (2017YFB1002502), in part by the National Natural Science Foundation of China (61701089), in part by the Natural Science Foundation of Henan Province of China (162300410333), and in part by the Fundamental Research Funds for the Central Universities (ZYGX2016J127).

ABSTRACT Biometric identity authentication technology is widely used in the field of information security. As a new biological method, electroencephalography (EEG) is gradually applied in biometric recognition, because scientists believe that practicability and portability are the development direction of EEG identity authentication. This work investigates the feasibility of using resting state EEG signals recorded by single-channel portable device for identity authentication. Single-channel EEG classification are effectively improved by using mixed-method in three feature domains (i.e., time, frequency, and time-frequency), feature selection (Rayleigh quotient) and classifier design (ensemble classifier). We invited 46 subjects to participate in the EEG identity authentication experiment. Experimental results show that the open-eyed resting state is an ideal authentication method, and the average classification accuracy of the authentication algorithm can reach 95.48% in 2 seconds, validating that the new method of processing single-channel EEG signals is especially useful in extrapolating EEG identity authentication to realistic field contexts.

INDEX TERMS EEG, identity authentication, portable, resting state, empirical mode decomposition, generalized Rayleigh quotient, ensemble classifier.

I. INTRODUCTION

Biometrics-based authentication methods have been an important research topic in the field of information security. Among biometrics technologies only electroencephalography (EEG) [1] signals reflect unique brain activity, thus providing a portable approach to low-cost and high-resolution [2] identity authentication.

EEG identity authentication has three prominent advantages: living, anti-coercion, and expandable attributes. Living attributes ensure that artifacts or amputated limbs cannot be authenticated because they cannot generate brain waves. The anti-coercion attribute endows users with tension and anxiety when they are threatened. By detecting the abnormal reaction of the brain, the system can use protective operation to maintain account security. Extended attributes can combine various EEG authentication methods, such as resting state, facial visual stimulus, and auditory name stimulus, to enhance system security.

EEG has the theoretical basis of biometric identification. Modern magnetic resonance imaging technology shows that people's brains not only have structural differences determined by genes but also functional differences due to the dissimilarities in people's memory, personality, and thinking modes. John Ratey proposed that the brain is variable, and long-term exercise can regulate brain balance and enhance neuronal connections. N Doidge's research also revealed that people's habits and hobbies can alter the structure and connection patterns of the brain. Verweij *et al.* [3] confirmed that exogenous factors affect EEG.

The associate editor coordinating the review of this manuscript and approving it for publication was Zehong Cao.

Several researchers explored the relationship between EEG and genes. Davis first studied the genotype–phenotype relationship between twins. Püschel *et al.* [4] believes that the resting-state characteristics of family members are more similar than those of unrelated individuals. In EEG frequency domain studies, De *et al.* [5] revealed that 8–16 Hz EEG frequencies are highly heritable. Further studies [6] showed that average spectral power and frequency values in the alpha and beta bands are highly heritable. Recent studies [7] discovered that the alpha power and peak frequency in the occipital region seem to exhibit strong heritability.

Basing on differences in brain structure, functional connectivity and heredity, Stassen [8] introduced the brain-print concept, which suggests the possibility of using EEG to authenticate identity. Subsequent research in this direction can be divided into two types: task-based and resting-state.

Task-based paradigms are mostly authenticated by event-related potentials (ERP) or steady-state visual evoked potentials (SSVEP). In the early applications of ERP, Yeom's team [9] used the N170 and N250 time-domain features to complete 10 user experiments, and the accuracy rate was 86.1%. Orlando Nieves's team [10] combined time and frequency-domain features to improve the accuracy of authentication to 90%. Additionally, several studies [11] attempted to extract multiple entropy [12] as features and use deep learning [13], [14] to improve classification accuracy. In SSVEP research, Cao *et al.* [15], [16]. found that inherent fuzzy entropy can objectively reflect the robustness and complexity of the brain [17], and proposed its reliability in various fuzzy entropy tests [18] [19], expanding the nonlinear feature representation of EEG signals.

Task-based identity authentication needs a display screen for stimulation, and is complex and time-consuming. Resting state experiments are simple, and the subjects maintain their resting states with open or closed eyes. Extensive research [20] explored the stability of resting EEG signals and proved the feasibility of resting EEG signals in multi-time span [21]. Most researchers agree that the results of identity authentication are influenced by electrode selection, frequency-domain rhythm [22]–[25] and time-frequency analysis [26]. Historically, some attempts [27], [28] were made to study the resting state of the single channel, but single-channel methods, which have low accuracy, have been gradually replaced by multichannel [29] methods. In a resting-state multichannel method, the use two or three [30], [31] channels is popular because of the acquisition convenience. Scientists also use neural networks [32] [33], [34] for EEG identity authentication, and 32 or 64 channels of EEG data are more suitable for deep learning. More recent attention [35]–[37] has been devoted to resting state brain networks and the connectivity of functional areas in resting states.

However, most previous studies were limited to improving classification accuracy. When the accuracy is guaranteed, few researchers paid attention to the practicability of identity authentication methods. Two main problems restrict the daily application of EEG identity authentication. First, multichannel wet electrode devices need 10 to 20 minutes of preparation time, and thus using them is infeasible in practice. Second, most task-based identity authentication methods are impractical for people with visual impairment.

This work aims to promote the practicability of EEG identity authentication in life, simplify the experimental process to the greatest extent and reduce time consumption. We use the resting state for convenience, and select a single-channel dry-electrode EEG acquisition device to reduce wearing time, and achieve fast and convenient daily use requirements. Compared with 16 and 32-channel devices, single-channel devices lack spatial information. Furthermore, average reference, spatial filtering and other noise reduction methods, which can affect the signal quality cannot be used. The stability analysis of single-channel equipment faces such problems. Special mean baseline correction is needed in the pretreatment stage. The problem of insufficient features must be solved by mixing multiple feature domains.

A mixed-method approach was employed in three stages: preprocessing, feature selection and classifier design. First, in the pre-processing stage, the mean of all data was used as the baseline of the signal to enhance the stability. Then, we extracted EEG features in three feature domains: time, frequency and time-frequency domains. A feature selection method based on Rayleigh quotient was proposed to select high quality features from the three feature domains. Finally, we used voting strategy-based ensemble classifier to reduce individual classifier errors. This research shows that using a single-channel device in the resting state can achieve 95.48% accuracy and reduce the time consumption to 2 seconds.

II. METHOD

A. EEG DATA ACQUISITION

Forty-six undergraduate and graduate students (i.e., 23 males and 23 females) with an average age of 22.64 years (range = 17–24, SD = 2.16) participated in our experiment. They were all right-handed students, with normal or corrected to normal visual acuity. None of the subjects had psychiatric disorders, such as neurological disorders, epilepsy, depression, and no history of drug abuse or other serious diseases. Before the experiment began, we obtained the participants' informed consent and the approval of the ethics committee of China National Digital Switching System Engineering and Technological Research Center. All of the subjects provided informed consent prior to the experiments and received a monetary compensation for participating in the experiment.

A portable device, MindWave Mobile [2], was used for EEG data acquisition via the forehead, as shown in Fig. 1. Wearing this single-channel device will greatly simplify the preparation process and improve comfort.

The EEG acquisition site was selected in a closed and quiet room, and the smart devices equipment of the subjects were removed so that the interference of the electromagnetic environment on the recorded signals was reduced. The left

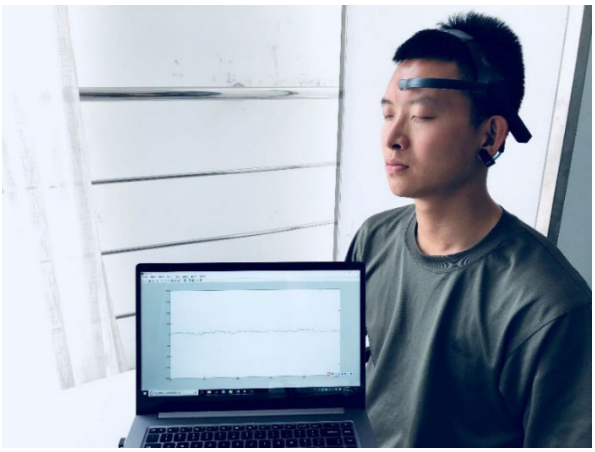

FIGURE 1. Collecting a subject's resting EEG data with MindWave mobile.

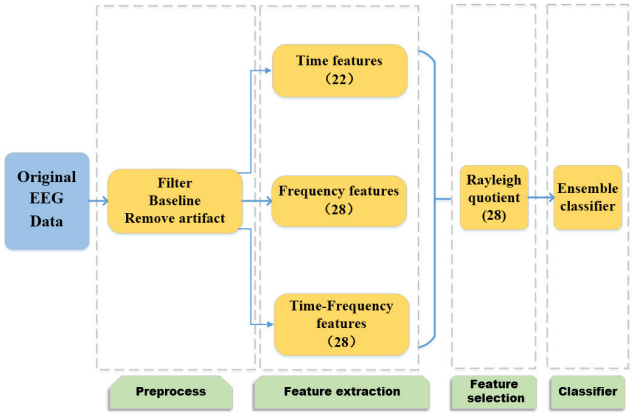

FIGURE 2. Framework of the EEG authentication system.

earlobe was used as the reference electrode of MindWave, and the dry electrode was placed on FP1 (i.e., 10-20 system) [38]. The subjects were instructed to relax but not to sleep, and try to avoid biting, swallowing, eye movement, crossing legs and other movements during the data acquisition process.

The sampling rate was 512 Hz. The total experiment period for each subject was 7 minutes. The entire acquisition process was divided into two blocks. In block-1, the participants were asked to open their eyes at rest for 3 minutes, whereas in block-2, the participants were required to close their eyes at rest for 3 minutes. One minute relaxation was performed between the two blocks.

B. DATA ANALYSIS

The pattern recognition method was applied on the single-channel resting EEG signals for identity authentication, as shown in Fig. 2. First, in the preprocessing stage, data quality was improved by filtering, baseline correction and artifact removal. Then, distinct features for individuals were extracted from the time, frequency and time-frequency domains. Rayleigh quotient was used for the reduction of redundancy and selection of the most suitable features for identity authentication. Finally, three independent classifiers, namely, KNN, LDA, and SVM, were trained, and an integrated classifier was designed based on a voting strategy.

TABLE 1. Linear characteristics.

Statistical features	Formula
Zero-crossing rate	$Z_X = \frac{1}{N} Z_{num}(x)$ $Z_{num}(x)$ *is the number of times a signal passes through the x−axis*
Mean	$\mu_X = \frac{1}{N}\sum_{i=1}^{N} x_i$
Standard deviation	$\sigma_X = \sqrt{\frac{1}{N}\sum_{i=1}^{N}(x_i - \mu_X)^2}$
Coefficient of variation	$\mathrm{Cv} = \frac{\sigma_X}{\mu_X}$
1st difference	$\delta_x = \frac{1}{N-1}\sum_{i=1}^{N-1}\lvert x_{i+1} - x_i\rvert$
2nd difference	$\gamma_x = \frac{1}{N-2}\sum_{i=1}^{N-2}\lvert x_{i+2} - x_i\rvert$
K-order origin distance	$V_k = \frac{1}{N}\sum_{i=1}^{N} x_i^k \quad (k = 3,4)$
K-order center distance	$C_k = \frac{1}{N}\sum_{i=1}^{N}(x_i - \mu_X)^k \quad (k = 3,4)$

1) PREPROCESSING

Preprocessing can effectively reduce EEG signal noise. The duration for each block was 180 seconds. The first 10 seconds in each block was removed. Artifacts were removed with a threshold of 90 μv. Chebyshev filter and zero-phase filtering were applied for 0–60 Hz low-pass filtering. Then, the data were segmented into 2 seconds without overlap. To improve the stability of the resting EEG signals, the averaged amplitude of each segment was used as the baseline for the data correction. The benefit of this approach is that the signal-to-noise ratio of the single-channel signal increased, and the useless data were eliminated.

2) FEATURE EXTRSCTION

a: TIME DOMAIN FEATURE EXTRACTION

Commonly used statistics features [39] were selected in the time domain, as shown in TABLE 1. Nonlinear features such as approximate entropy, sample entropy and 8-order AR model parameters were used. The preprocessed EEG signal was $x = (x_1, x_2, x_3 \ldots x_N)$, and the signal length was N.

In recent years, the nonlinear analysis of EEG signals has been widely used [18]. We used approximate entropy and sample entropy to calculate the complexity of unstable time series. m was set to 2 or 3 in the two methods.

The correlation parameters of approximate entropy [40] were m and r, and m was the vector length during comparison.

In this experiment, the lengths of m were 2 and 3, respectively. Parameter r represented the threshold of similarity, and $r = 0.2 \times \sigma_X$ was selected for the experiment. The EEG data $x = (x_1, x_2, x_3 \ldots x_N)$ was reconstructed into vector $U(1), U(2), U(3), \ldots, U(N - m + 1)$, where $U(i) = [x_i, x_{i+1}, \ldots, x_{i+m-1}]$, $d[U(i), U(j)]$ was defined as the maximum distance of the corresponding location element in $U(i)$, $U(j)$ vector. $num(ui)$ was used to represent the number of $d[U(i), U(j)] < r$, and $j = i$ was allowed.

$$A_i^m(r) = \frac{1}{N-m+1} num(ui) \tag{1}$$

$$\Psi^m(r) = \frac{1}{N-m+1} \sum_{i=1}^{N-m+1} \ln(A_i^m(r)) \tag{2}$$

Approximate entropy is defined as

$$\text{apen(m,r)} = \Psi^m(r) - \Psi^{m+1}(r) \tag{3}$$

Sample entropy and approximate entropy are similar in physical meaning. Sample entropy has two advantages: the value of sample entropy is independent of the signal length, and sample entropy has good consistency. As an improvement method of approximate Entropy. Sample entropy and approximate entropy have two differences, $j \neq i$ in calculating distance. The comparison with its own data is cancelled. In the equation $\Psi^m(r) = \frac{1}{N-m+1} \sum_{i=1}^{N-m+1} A_i^m(r)$, logarithmic computation is cancelled. Finally, the logarithmic calculation is added to sampen(m,r) $= -\ln(\frac{\Psi^{m+1}(r)}{\Psi^m(r)})$ when the sample entropy is defined. The calculated length can be precisely defined as the difference of $\Psi^m(r)$ between m and $m + 1$.

In addition, given that EEG is not a completely random signal and the information is correlated in the signal, using the AR model [41] in the design of a linear filter can approximate the generation process of an EEG signal. The AR process can be approximated to an EEG signal by establishing a channel model with an autoregressive algorithm. We set the order of the AR model to 8 and used the fitted model coefficients as features. $x(n)$ is the input signal, $y(n)$ is the output signal, $X(z)$ and $Y(z)$ are the Z-transform of $x(n)$ and $y(n)$, respectively, and $H(z)$ is the Z-transform of system response function.

The AR model is built as follows:

$$y(n) = x(n) - \sum_{i=1}^{p} a_i y(n-i), \quad a_p \neq 0 \tag{4}$$

The system response of the AR model can be obtained as follows:

$$H(z) = \frac{Y(z)}{X(z)} = \frac{1}{\sum_{i=0}^{p} a_i z^{-i}} = \frac{1}{A(z)} \tag{5}$$

By using Yule-Walker equation to solve AR model coefficients, the final calculated $a_1, a_2, \ldots, a_8$ was taken as the feature of the EEG time domain.

TABLE 2. Five rhythms of EEG.

EEG rhythm	Frequency range(Hz)	State
δ	0.5-4	Deep sleep
θ	4-8	Mental relaxation
α	8-14	Clear-headed
β	14-30	Brain awakening and alertness
γ	30-60	High frequency

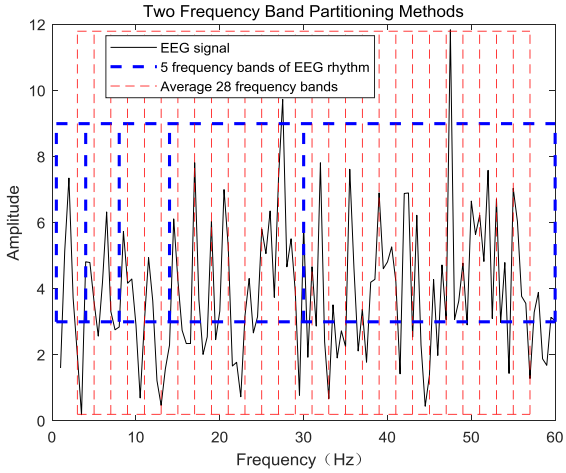

FIGURE 3. Illustration of AFB method and traditional 5-rhythm frequency band method.

b: FREQUENCY DOMAIN FEATURE EXTRACTION

Traditional methods [42] divide EEG signals into five rhythms of $\delta, \theta, \alpha, \beta, \gamma$ in the range of 0–60Hz, as shown in TABLE 2.

However, this method of frequency band division is extremely rough to clearly capture individual differences. Moreover, if each rhythm calculates one feature, then only five frequency domain features can be obtained by a single-channel device, resulting in insufficient number of features, increasing the difficult of the classifier in identifying legal users.

Hence, we proposed a method of uniformly dividing the frequency domain to extract detailed frequency features. The average frequency band (AFB) method was used in this work. We divided 3–58 Hz into 28 parts, and the size of each frequency band was $\Delta f = 2Hz$, as shown in Fig. 3. The energy characteristics for each frequency band were calculated as the differential entropy (DE) as follows:

$$DE = \log(\int_R X(w)^2) \tag{6}$$

$X(w)$ is the Fourier transform of data band $X(n)$, and R is the frequency range of sub-band.

c: TIME-FREQUENCY DOMAIN FEATURE EXTRACTION

The empirical mode decomposition (EMD) algorithm can decompose itself through its own signal waveform, without relying on any basis function. Studies [43] have proposed that

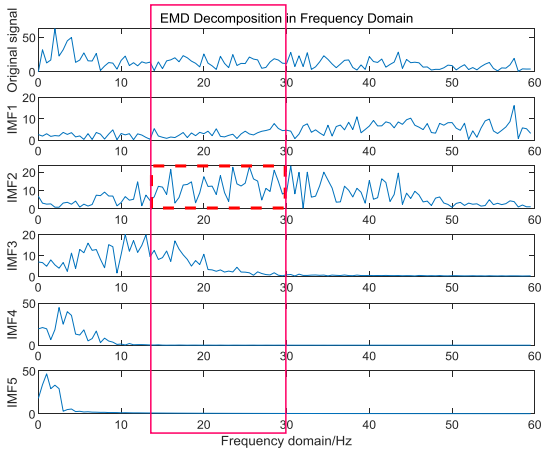

FIGURE 4. EMD decomposition of original resting EEG signals.

this method can be used to deal with nonstationary nonlinear signals. Data can be decomposed into multilayer intrinsic mode function (IMF) by the EMD algorithm:

$$x(t) = \sum_{n=1}^{N} IMF_n + r \tag{7}$$

Different filtering [44] effects can be obtained by adjusting different layers of IMF. Fig. 4 shows five IMFs decomposed from the original resting EEG data. This figure shows that the main component of IMF-2 consists of the beta rhythm. Given that existing studies have provided evidence of the distinct of beta frequencies for human EEG related to specific sensorimotor cortical areas, so we mainly focused on the IMF-2 to extract identity features. Fourier- transform was performed on IMF-2. Then differential entropy was calculated for each frequency band uniformly divided from 3–58 Hz.

3) RAYLEIGH QUOTIENT BASED FEATURE SELECTION

We extracted features as personal identity characteristics from the time (22 features), frequency (28 features) and time-frequency domains (28 features). In the time domain, 22 features with different methods and parameters were extracted, and 11 of these linear features are shown in Table 1. Among the nonlinear features, two are of sample entropy, two are of approximate entropy and seven are of the AR model parameters. In the frequency and time-frequency domains, the features were computed by the AFB method. Each of the two feature domains has 28 energy features. However, redundancy [45] was observed among these features. For identity authentication, the features should be stable within each subject's data and distinct [46] for each subject. We proposed a Rayleigh quotient (RQ) based feature selection method for redundancy reduction and the selection of the most suitable features from the multi-domain. RQ is calculated by dividing the between-class distance by the within-class distance. The features of the large between-class distance and small within-class distance make setting thresholds easy for classifiers.

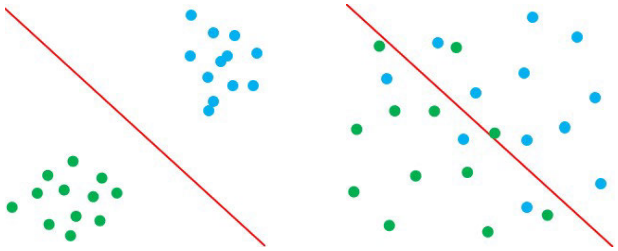

FIGURE 5. Feature distribution of different rayleigh quotients.

In the RQ [47] calculation of two features, the characteristics are $t_{11}, t_{12}, t_{13} \ldots, t_{1n}$ or $t_{21}, t_{22}, t_{23} \ldots, t_{2n}$. The mean values of the two features are M_1, M_2, the variances of the two features are S_1, S_2, the intra-class distance is $S_w = S_1 + S_2$, and the inter-class distance is $S_b = (M_1 - M_2)^2$.

Then the RQ formula of the two features is:

$$J_R = \frac{(M_1 - M_2)^2}{S_1 + S_2} = \frac{S_b}{S_w} \tag{8}$$

The generalized the RQ [48] calculation with multiple features, it can be transformed into a matrix form:

$$J_R(\vec{w}) = \frac{between - class\ distance}{within - class\ distance} = \frac{\sum_{j=1}^{n}\sum_{i=1}^{n}(M_i - M_j)^2}{\sum_{i=1}^{n} S_i} = \frac{\vec{w}^T S_b \vec{w}}{\vec{w}^T S_w \vec{w}} \tag{9}$$

Fig. 5 presents a clustering diagram of the high and low RQ features. The small RQ features were dispersed, making the classification boundary difficult to determine, and thus increasing the probability of error classification. On the contrary, classification accuracy can be improved by selecting large RQ features.

The RQs of 78 features in the three feature domains were ranked from large to small, and the top 28 features with the largest RQ value were selected as the high quality features.

4) ENSEMBLE LEARNING-BASED CLASSIFICATION

Ensemble learning accomplishes classification tasks by merging the results of multiple classifiers. First, multiple "single classifiers" are generated, then the results are integrated through different strategies. The ensemble classifier can correct the errors of a single classifier by the voting decision method. The category with the largest number of votes is the result of classification, according to the principle that the minority is subordinate to the majority.

The ensemble classifier must to satisfy two conditions: (1) The individual classifier has a better classification effect, otherwise it will reduces the ensemble effect. (2) Individual classifiers are as independent as possible, otherwise the integration effect is not obvious. Thus we selected KNN [49],

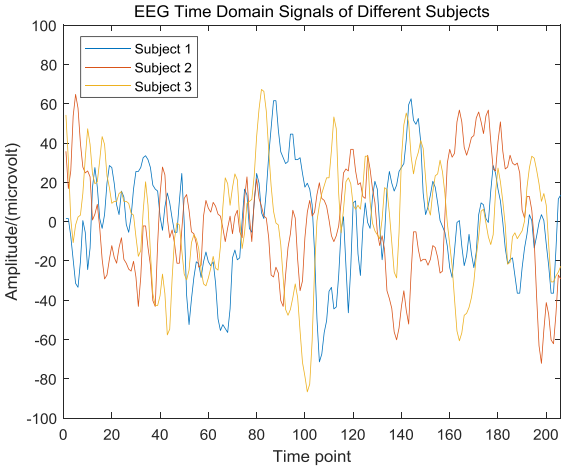

FIGURE 6. EEG time domain signals of different subjects.

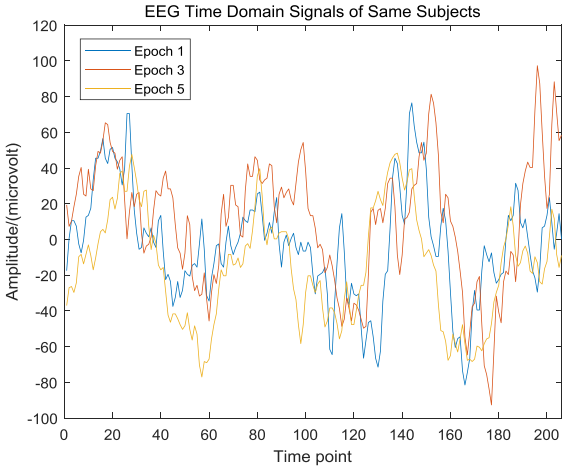

FIGURE 7. EEG time domain signals of the same subject.

LDA [50] and SVM [51] as individual classifiers with different classification algorithms.

For the KNN classifier, we used the fitcknn function in MATLAB and set parameters (Distance='Euclidean', NumNeighbors=3). For the LDA classifier, we used the fitcdiscr function in MATLAB and set the parameter (DiscrimType=linear). For the SVM classifier, we used the libsvm toolbox and the radial basis function (RFB) as the kernel function.

In this experiment, we designed personal-based classifiers for each participant. The mean of 46 personal classifiers was considered as the classification performance of the overall identity authentication system. The personal classifier has two kinds of labels, samples of one subject (label 1) and an equivalent sample randomly selected from the remaining 45 users (label 2). We used fivefold cross validation to calculate the accuracy, and recorded false positive rate(FPR) and false negative rate(FNR).

III. RESULT

A. TIME-DOMAIN AND FREQUENCY-DOMAIN WAVEFORMS

The waveforms in the time and frequency domains determine the quality of extracted features. The stability of EEG signals can be analyzed by drawing waveforms of the same subjects in different time epochs, and drawing the waveforms of different subjects can analyze the differences among signals.

The time domain results are shown in Fig.6 and Fig.7. Apparently, the time domain waveform varies greatly among different subjects (Fig. 6), but the waveform stability of the subjects is poor (Fig.7). Given the poor signal stability, the statistical features [38] in the time domain are more suitable for resting EEG signals than detailed features.

The frequency domain results are shown in the following figure. The waveforms of different users are obviously different in the frequency domain (Fig. 8). Signals in a single subject vary in stability in the time and frequency domains. Obviously, the frequency domain features (Fig. 7) have higher similarity than the time domain features (Fig. 9). On the basis of the four figures, we can conclude that the frequency domain is better in terms of discrimination and the self-stability of subjects.

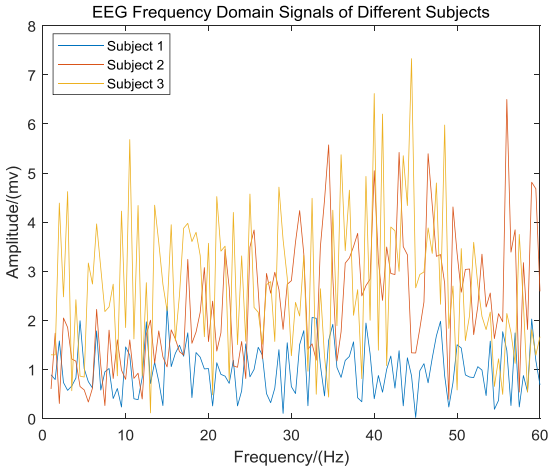

FIGURE 8. EEG frequency domain signals of different subjects.

B. PREPROCESSING

Baseline correction is an important step in data preprocessing. Baseline correction can reduce signal drift, usually by subtracting a constant from original data. Traditional methods always use the average amplitude of data before each epoch as the baseline. Given that resting state EEG signals are unstable and nearly unpredictable, we proposed that use of the average amplitude of all data in each epoch as the baseline.

To demonstrate average amplitude of all data's baseline performance, we compared the correlation between the same features extracted from data by using two different baseline correction methods. We calculated the Pearson correlation coefficients of the features from two adjacent data after baseline correction. The correlation of the same feature was recorded as self- correlation, and the correlation of different

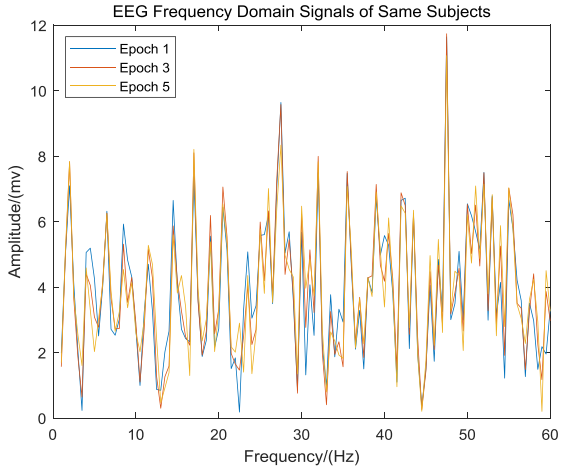

FIGURE 9. EEG frequency domain signals of the same subject.

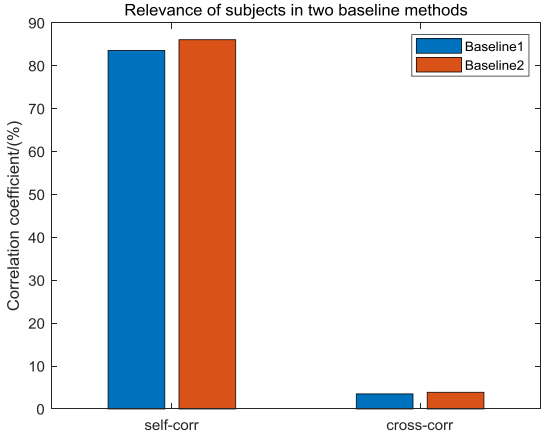

FIGURE 10. Comparison of self-correlation and cross-correlation coefficients using two different baselines.

features was recorded as cross- correlation. Fig.10 shows the result of the comparison between self-correlation and cross-correlation coefficients on the basis of two different baselines, which are the averaged amplitude of data before each epoch (Baseline 1) and averaged amplitude of each epoch (Baseline 2). The results show that the cross-correlation of the two baselines are at the same level. However, the self- correlation of Baseline 2 is higher than that of Baseline 1, indicating that the features processed by Baseline 2 have good similarity at different times. Fig. 10 suggests that Baseline 2 is more suitable for the resting EEG data, and the averaged amplitude of each epoch can improve the features' stability.

Fig.11 shows the classification results of the two baselines. The features of the two baselines were tested using the KNN, LDA and SVM classifiers. The result indicates that the SVM classifier has the highest accuracy, and using the averaged amplitude of each epoch as the baseline can significantly improve the classification accuracy of the three classifiers.

C. FEATURE EVALUATION

For identity authentication, features should be able to describe individual differences, that is, features of different

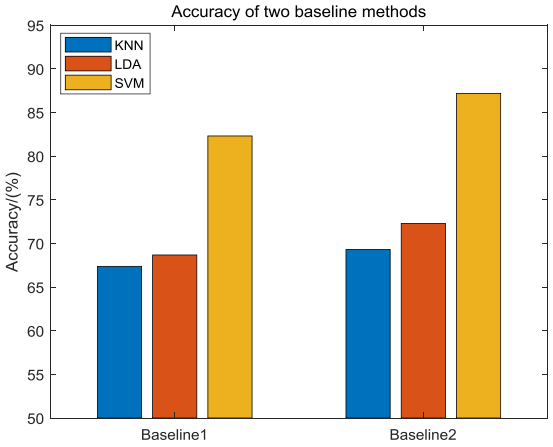

FIGURE 11. Comparison of the classification performance with two different baselines.

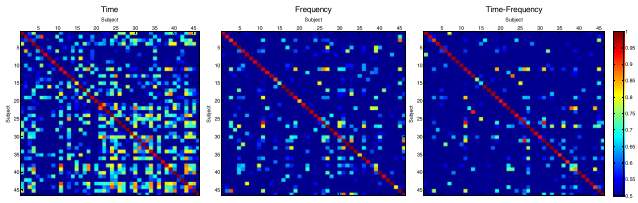

FIGURE 12. The correlation coefficient matrices of the subjects' features in three feature domains.

subjects should be significantly different. Meanwhile, the features of the same subject should be stable and unchanged with time. We calculated the correlation coefficient matrix to analyze three characteristic domains.

Fig.12 shows the correlation matrix of features between subjects. For each subject, features were extracted from the two continuous 25th and 26th epochs in the time, frequency and time-frequency domains. Then, feature correlation between subjects was calculated. The color of the square in the matrix represents the correlation coefficients of the two feature vectors between subjects. The matrix diagonals represent the subjects' self-correlation, and the other regions are the cross-correlation between subjects. The results show that features in the frequency and time-frequency domains have higher self-correlation coefficients and lower cross-correlation coefficients than those in the time domain, indicating that features in the frequency and the time-frequency domains are more stable and less redundant.

We traind KNN, LDA and SVM classifiers by using features extracted from three feature domains. The accuracy results are shown in Fig. 13. The classification effects of different classifiers vary, the classification accuracy of IMF-2 features in LDA and SVM was the highest, and the accuracy of using SVM classifier reaches 90%. Considering the results of Fig. 12, we believe that the stability and discrimination of features are important to the improvement of the classification accuracy.

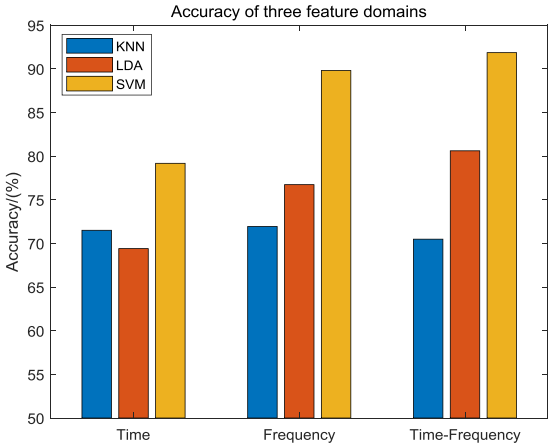

FIGURE 13. Classification results of different feature domains.

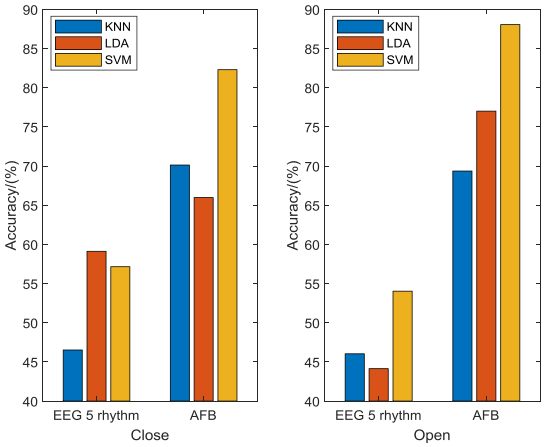

FIGURE 15. Comparison of classification accuracy using different frequency resolutions.

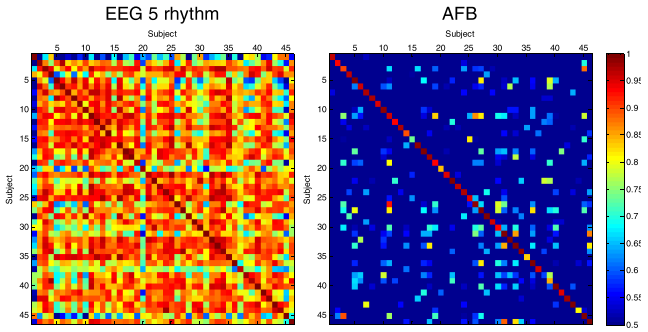

FIGURE 14. The correlation coefficient matrix of features between subjects for different frequency resolutions.

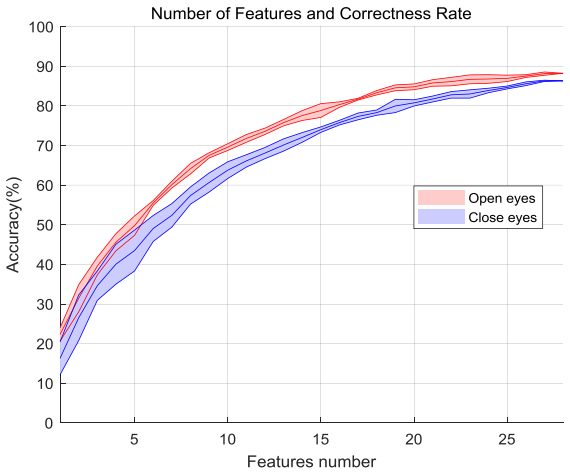

FIGURE 16. Number of features and classification accuracy.

D. FEATURE SELECTION

To reduce the feature dimension and obtain high quality features, we used the frequency domain as an example to study the optimal number of features.

We evaluated the features extracted from the frequency domain using different frequency resolutions (5 rhythms of EEG and uniformly divided 28 bands). The correlation coefficient matrix of the features between subjects are shown in Fig.14. The results, show that the self-correlations are relatively the same and high in for the two frequency resolutions, indicating that the frequency features are stable in the subjects. However, compared with the EEG 5 rhythms, a fine frequency resolution (2 Hz) can significantly reduce the correlation between subjects, indicating more disguisable between subjects.

The results of the three classifiers under the open-eye and closed-eye states are shown in Fig. 15. Classification accuracy in KNN, LDA, and SVM can be significantly improved by using a fine frequency resolution ($\Delta f = 2Hz$).

We found that the frequency features' resolution and quantity greatly influence accuracy. To explore the optimal number of selected features, we divided the 3–58 Hz frequency domain as evenly as possible into 1 to 28 bands with resolutions ranging from $\Delta f = 58Hz$ to $\Delta f = 2Hz$.

Fig.16, shows that the accuracy of resting eyes open is always higher than that of resting eyes closed. The accuracy improved with the increase in the number of features. Fig.16 shows that the improvement of the frequency feature resolution and feature dimension plays a positive role in classification and identification. When the number of features is higher than 25, the accuracy tends to stop increasing, indicating that increase in the number of features alone is not a continuous improvement of accuracy. On the basis of the above experimental results, we set the optimal number of feature selection to 28.

As mentioned above, the RQ was used for the selection of the best subset of features. Given the difference among features, the min–max normalization method was used in the mapping of features uniformly distributed from 0 to 1:

$$x_{Normalization} = \frac{x - X_{\min}}{x - X_{\max}} \tag{10}$$

TABLE 3 shows the result of the selected features. A total of 28 features with the highest RQ were chosen from the 78 features. The results show that the number of different

TABLE 3. The top 28 features with the highest rayleigh quotient.

Sort	Open		Close	
	Features	Rayleigh quotient	Features	Rayleigh quotient
1	4-order center distance	13.8789	4-order center distance	15.7547
2	4-order origin distance	11.7964	4-order origin distance	12.9986
3	3-order origin distance	11.9544	CV	12.1717
4	CV	10.5598	3-order center distance	11.9941
5	Freq 9-10(Hz)	10.0715	AR(8)-5	10.1315
6	IMF 45-46 (Hz)	9.6762	Freq 53-54(Hz)	8.3798
7	Freq 5-6(Hz)	9.3950	IMF 51-52(Hz)	8.0914
8	IMF 17-18(Hz)	9.2293	IMF 41-42(Hz)	8.0934
9	IMF 33-34 (Hz)	7.9880	Freq 25-26(Hz)	7.9999
10	Freq 15-16 (Hz)	7.4689	Std	7.4795
11	AR(8)-7	7.5049	Freq 37-38(Hz)	7.3470
12	IMF 41-42 (Hz)	7.2408	IMF 57-58(Hz)	7.3272
13	Freq 39-40(Hz)	7.1604	Freq 5-6(Hz)	6.8372
14	IMF 35-36 (Hz)	7.2930	Freq 13-14 (Hz)	6.4988
15	IMF 55-56(Hz)	6.9299	Freq 33-34 (Hz)	6.6364
16	IMF 43-44 (Hz)	6.8979	IMF 31-32(Hz)	6.3331
17	Freq 37-38 (Hz)	6.9242	AR(8)-3	6.4705
18	Freq 3-4(Hz)	6.8565	Apen(2)	6.0870
19	Apen(3)	6.7794	Freq 9-10 (Hz)	6.0355
20	IMF 13-14 (Hz)	6.4492	Freq 21-22(Hz)	6.0628
21	IMF 57-58(Hz)	6.3893	IMF 13-14(Hz)	5.9090
22	IMF 15-16 (Hz)	6.5103	Freq 3-4(Hz)	5.9126
23	IMF 31-32 (Hz)	6.3688	IMF 11-12(Hz)	5.8311
24	AR(8)-6	6.1729	IMF 53-54(Hz)	5.6820
25	Freq 7-8 (Hz)	5.7654	IMF 47-48(Hz)	5.5904
26	Freq 33-34 (Hz)	5.8939	Freq 29-30(Hz)	5.4969
27	IMF 23-24 (Hz)	5.7800	IMF 33-34(Hz)	5.5480
28	IMF 29-30 (Hz)	5.7903	IMF 45-46(Hz)	5.4764
mean		**7.8831**		**7.6492**

feature domains of the two resting states is 7:8:13 and 8:10:10 in the time, frequency and time-frequency domains, respectively. The rate at which the features in the frequency and time-frequency domains are selected is higher than that at which the features in the time domain is selected, whereas the time domain features have the highest RQs. Among the frequency and time-frequency features selected by the RQ method, beta and gamma frequency bands account for a large proportion because the amplitude of the beta band is larger in the resting state, and the gamma band is a related band. This may indicate that the features from the multi-domain are complementary to each other and capture the individual's identity information from different aspects. Moreover, we found that the mean RQ for features extracted from the eyes open resting EEG data is higher than that from the eyes closed resting state, suggesting that the eyes open resting EEG data contain more identity information of each subject.

AR(8)-4 represents the fourth coefficient in the 8-order AR model in the time domain.

Apen(3) represents the approximate entropy in the time domain where m equals 3.

Freq 51-52 (Hz) represents the 51-52 Hz energy features calculated in the frequency domain using the AFB method.

IMF 31-32 (Hz) represents the 31-32 Hz energy features calculated in the time-frequency domain through the AFB method

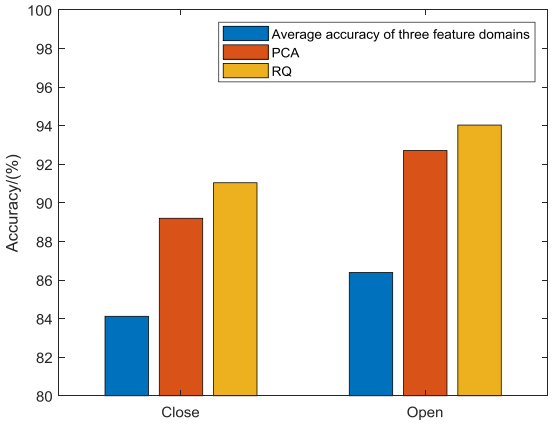

FIGURE 17. Accuracy of different feature selection methods.

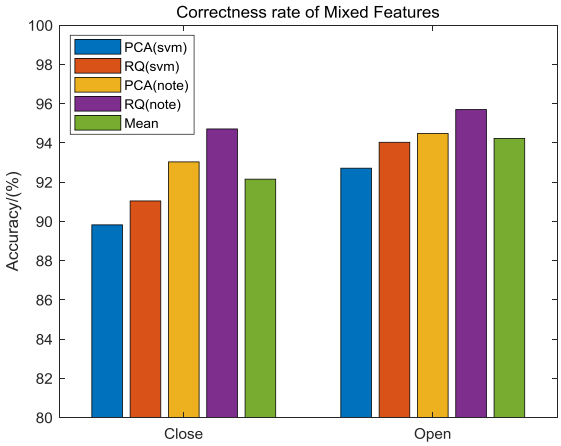

FIGURE 18. Classification results of ensemble classifiers.

Given that principal component analysis (PCA) is a traditional method for feature dimension reduction, PCA was also used to reduce the 78 features to 28 dimensions. Furthermore, to verify the effect of feature selection, the features extracted from each domain were used for separately classification and their averaged accuracy were compared with those using PCA and RQ-based feature selection. Fig.17 shows the comparison of classification accuracy under the eyes open and eyes closed resting states. PCA and RQ based feature selection method significantly improve the classification accuracy. The RQ-based feature selection's accuracy reaches 94% under the eyes open resting state. The RQ-based feature selection has higher classification accuracy than PCA-based method under the two resting states. The result reveals the importance of feature selection and the superiority of our proposed RQ-based feature selection method.

E. CLASSIFICATION

The previous experimental results present the individual classifier results, and the SVM exhibits the best classification performance. The features selected by the PCA and RQ methods are entered into the ensemble classifier as shown in Fig.18.

TABLE 4. Feature selection and ensemble classifier results.

Resting state	Feature selection and classification accuracy（%）		
	SVM	Ensemble classifier	**Mean**
Open (PCA)	93.95	94.21	**94.41**
Open (RQ)	94.62	95.48	
Close (PCA)	89.34	91.95	**92.38**
Close (RQ)	93.09	95.09	

TABLE 5. Comparisons with previous papers.

Author	Year	Subjects number	Time cost(s)	Electrode number	Protocol	Features	Accuracy (%)
Orlando Nieves et al [10]	2016	20	Not mention	2	Thinking movement	Time frequency	90
Zhendong Mu et al. [52]	2016	10	1	2	Visual Stimuli	Fuzzy entropy	87.3
Chisei Miyamoto et al [24]	2009	23	6	1	rest	Alpha	79
Kavitha P Thomas et al.	2017	6	4	14	rest	Alpha, beta, gamma	88.33
Ga-Young Choi et al.	2018	17	15	32	rest	Alpha	88.4
This paper	**2019**	**46**	**2**	**1**	**rest**	**Time Frequency IMF-2**	**95.48%**

Fig.18 indicates that the ensemble classifier has the best classification results. The voting strategy can reduce the classification interference of a single classifier and correct the errors of individual classifiers. After the features selected based on the RQ and the ensemble classifier are used, the averaged classification accuracy reaches the highest value 95.48% (FPR=3.77%, FNR=5.27%) under the eyes open resting state. Furthermore, accuracy of the ensemble classifier is higher than that of the SVM classifier by 1%.

TABLE 4 presents that the classification results of the 46 subjects' data sets. Classification performance under the eyes open resting state was better than that under the eyes closed resting state. This result indicates that the eyes open resting state EEG may involve many conscious activities recorded by the frontal electrode, which is essentially helpful for identity authentication.

IV. DISCUSSION

With the development of brain science in the field of identity authentication, various stimuli have been used for identity recognition. TABLE 5 presents the comparison between our study with the achievements with regard to the use of EEG in identity authentication in recent years. Our method has certain advantages in different aspects. In terms of the number of subjects, we collected 92 times resting data from 46 subjects and constructed a database with sufficient samples. We selected the resting state, which is the simplest task state, not only for convenience and practicability, but also for addressing signal the fluctuation. In terms of time consumption, 2 seconds of authentication time approaching daily requirements. In resting state, we consumed the shortest time, indicating the convenience and practicability of our method. Reducing the number of electrodes to one can minimize the preparation time. The comparison of the final correct rates indicates that our correct rate can exceed 95%, confirming the effectiveness of the authentication system.

V. CONCLUSION

To simplify the process of EEG identity authentication and increase operability, work selected the resting state and used a single-channel device with dry electrodes. Mixed methods were used in the experiment, and stability and accuracy were improved significantly through the average amplitude baseline method, three feature domains extraction, RQ feature selection and ensemble classifier design. The results show that 28 features can maintain classification accuracy and reduce data dimension, and the open-eye state has a higher accuracy than the closed-eye state. The EEG identity authentication method in this experiment can reach 95.48%.

Although EEG is affected by emotions, sleep and other factors in practical applications, the electromagnetic environment and interference in reality is difficult to predict. However, this work provides an effective method for the data processing stage, increasing the feasibility of extending the EEG identity authentication from laboratory to real life.

REFERENCES

[1] H. H. Stassen, G. Bomben, and P. Propping, "Genetic aspects of the EEG: An investigation into the within-pair similarity of monozygotic and dizygotic twins with a new method of analysis," *Electroencephalogr. Clin. Neurophysiol.*, vol. 66, pp. 489–501, Jun. 1987.
[2] M. D. Pozo-Banos, J. B. Alonso, J. R. Ticay-Rivas, and C. M. Travieso, "Electroencephalogram subject identification: A review," *Expert Syst. Appl.*, vol. 41, no. 15, pp. 6537–6554, 2014.
[3] K. J. H. Verweij, S. N. Shekar, B. P. Zietsch, L. J. Eaves, J. M. Bailey, D. I. Boomsma, and N. G. Martin, "Genetic and environmental influences on individual differences in attitudes toward homosexuality: An australian twin study," *Behav. Genet.*, vol. 38, pp. 257–265, May 2008.
[4] J. Püschel, H. H. Stassen, G. Bomben, C. Scharfetter, and D. Hell, "Speaking behavior and speech sound characteristics in acute schizophrenia," *J. Psychiatric Res.*, vol. 32, no. 2, p. 89, 1998.
[5] L. De Gennaro, F. Fratello, C. Marzano, F. Moroni, G. Curcio, D. Tempesta, M. C. Pellicciari, C. Pirulli, M. Ferrara, and P. M. Rossini, "Cortical plasticity induced by transcranial magnetic stimulation during wakefulness affects electroencephalogram activity during sleep," *PLoS ONE*, vol. 3, no. 6, p. e2483, 2008.
[6] S. E. Eischen, J. Y. Luckritz, and J. Polich, "Spectral analysis of EEG from families," *Biol. Psychol.*, vol. 41, p. 61, Aug. 1995.
[7] B. P. Zietsch, J. L. Hansen, N. K. Hansell, G. M. Geffen, N. G. Martin, and M. J. Wright, "Common and specific genetic influences on EEG power bands delta, theta, alpha, and beta," *Biol. Psychol.*, vol. 75, pp. 154–164, May 2007.
[8] H. H. Stassen, "Computerized recognition of persons by EEG spectral patterns," *Electroencephalogr. Clin. Neurophysiol.*, vol. 49, pp. 190–194, Jul. 1980.
[9] S.-K. Yeom, H.-I. Suk, and S.-W. Lee, "Person authentication from neural activity of face-specific visual self-representation," *Pattern Recognit.*, vol. 46, no. 4, pp. 1159–1169, 2013.
[10] O. Nieves and V. Manian, "Automatic person authentication using fewer channel EEG motor imagery," in *Proc. World Automat. Congr.*, Jul./Aug. 2016, pp. 1–6.
[11] T. Pham, W. Ma, D. Tran, P. Nguyen, and D. Phung, "A study on the feasibility of using EEG signals for authentication purpose," in *Proc. Int. Conf. Neural Inf. Process.*, 2013, pp. 562–569.
[12] Z. Mu, J. Hu, J. Min, and J. Yin, "Comparison of different entropies as features for person authentication based on EEG signals," *IET Biometrics*, vol. 6, no. 6, pp. 409–417, Nov. 2017.
[13] Q. Wu, B. Yan, Y. Zeng, C. Zhang, and L. Tong, "Anti-deception: Reliable EEG-based biometrics with real-time capability from the neural response of face rapid serial visual presentation," *Biomed. Eng. OnLine*, vol. 17, no. 1, p. 55, 2018.
[14] Q. Gui, Z. Jin, and W. Xu, "Exploring EEG-based biometrics for user identification and authentication," in *Proc. IEEE Signal Process. Med. Biol. Symp.*, Dec. 2015, pp. 1–6.

[15] Z. Cao, K.-L. Lai, C.-T. Lin, C.-H. Chuang, C.-C. Chou, and S.-J. Wang, "Exploring resting-state EEG complexity before migraine attacks," *Cephalalgia*, vol. 38, no. 7, pp. 1296–1306, 2017.
[16] Z. Cao, W. Ding, Y.-K. Wang, F. K. Hussain, A. Al-Jumaily, and C.-T. Lin, "Effects of repetitive SSVEPs on EEG complexity using multi-scale inherent fuzzy entropy," *Neurocomputing*, to be published.
[17] Z. Cao, M. Prasad, and C.-T. Lin, "Estimation of SSVEP-based EEG complexity using inherent fuzzy entropy," in *Proc. IEEE Int. Conf. Fuzzy Syst.*, Jul. 2017, pp. 1–5.
[18] Z. Cao, C.-T. Lin, K.-L. Lai, L.-W. Ko, J.-T. King, K.-K. Liao, J.-L. Fuh, and S.-J. Wang, "Extraction of SSVEPs-based inherent fuzzy entropy using a wearable headband EEG in migraine patients," *IEEE Trans. Fuzzy Syst.*, to be published.
[19] Z. Cao and C.-T. Lin, "Inherent fuzzy entropy for the improvement of EEG complexity evaluation," *IEEE Trans. Fuzzy Syst.*, vol. 26, no. 2, pp. 1032–1035, Apr. 2018.
[20] E. Maiorana, D. L. Rocca, and P. Campisi, "On the permanence of EEG signals for biometric recognition," *IEEE Trans. Inf. Forensics Security*, vol. 11, no. 1, pp. 163–175, Jan. 2015.
[21] S. Altahat, M. Wagner, and E. M. Marroquin, "Robust electroencephalogram channel set for person authentication," in *Proc. IEEE Int. Conf. Acoust., Speech Signal Process.*, Apr. 2015, pp. 997–1001.
[22] S. Altahat, G. Chetty, D. Tran, and W. Ma, "Analysing the robust EEG channel set for person authentication," in *Neural Information Processing*. Cham, Switzerland: Springer, 2015.
[23] I. Nakanishi, S. Baba, and C. Miyamoto, "EEG based biometric authentication using new spectral features," in *Proc. Int. Symp. Intell. Signal Process. Commun. Syst.*, Jan. 2009, pp. 651–654.
[24] C. Miyamoto, S. Baba, and I. Nakanishi, "Biometric person authentication using new spectral features of electroencephalogram (EEG)," in *Proc. Int. Symp. Intell. Signal Process. Commun. Syst.*, Feb. 2009, pp. 1–4.
[25] K. P. Thomas and A. P. Vinod, "Utilizing individual alpha frequency and delta band power in EEG based biometric recognition," in *Proc. IEEE Int. Conf. Syst., Man, Cybern.*, Oct. 2017, pp. 4787–4791.
[26] M. DelPozo-Banos, C. M. Travieso, C. T. Weidemann, and J. B. Alonso, "EEG biometric identification: A thorough exploration of the time-frequency domain," *J. Neural Eng.*, vol. 12, no. 5, 2015, Art. no. 056019.
[27] M. Poulos, M. Rangoussi, V. Chrissikopoulos, and A. Evangelou, "Person identification based on parametric processing of the EEG," in *Proc. IEEE Int. Conf. Electron., Circuits Syst.*, Sep. 1999, pp. 283–286.
[28] R. B. Paranjape, J. Mahovsky, L. Benedicenti, and Z. Koles, "The electroencephalogram as a biometric," in *Proc. Can. Conf. Elect. Comput. Eng.*, May 2001, pp. 1363–1366.
[29] A. Riera, A. Soria-Frisch, M. Caparrini, C. Grau, and G. Ruffini, "Unobtrusive biometric system based on electroencephalogram analysis," *EURASIP J. Adv. Signal Process.*, vol. 2008, Jan. 2007, Art. no. 18.
[30] P. Campisi, G. Scarano, F. Babiloni, D. V. Fallani, S. Colonnese, and E. Maiorana, "Brain waves based user recognition using the 'eyes closed resting conditions' protocol," in *Proc. IEEE Int. Workshop Inf. Forensics Secur.*, Nov./Dec. 2011, pp. 1–6.
[31] D. L. Rocca, P. Campisi, and G. Scarano, "EEG biometrics for individual recognition in resting state with closed eyes," in *Proc. Int. Conf. Biometrics Special Interest Group*, Sep. 2012, pp. 1–12.
[32] R. Palaniappan, "Method of identifying individuals using VEP signals and neural network," *IEE Proc.-Sci., Meas. Technol.*, vol. 151, no. 1, pp. 16–20, Jan. 2004.
[33] G.-Y. Choi, S.-I. Choi, and H.-J. Hwang, "Individual identification based on resting-state EEG," in *Proc. Int. Conf. Brain-Comput. Interface*, Jan. 2018, pp. 1–4.
[34] L. Ma, J. W. Minett, T. Blu, and W. S.-Y. Wang, "Resting state EEG-based biometrics for individual identification using convolutional neural networks," in *Proc. Annu. Int. Conf. IEEE Eng. Med. Biol. Soc.*, Aug. 2015, pp. 2848–2851.
[35] M. Fraschini, A. Hillebrand, M. Demuru, L. Didaci, and G. L. Marcialis, "An EEG-based biometric system using eigenvector centrality in resting state brain networks," *IEEE Signal Process. Lett.*, vol. 22, no. 6, pp. 666–670, Jun. 2015.
[36] D. J. A. Smit, C. J. Stam, D. Posthuma, D. I. Boomsma, and E. J. C. de Geus, "Heritability of 'small-world' networks in the brain: A graph theoretical analysis of resting-state EEG functional connectivity," *Hum. Brain Mapping*, vol. 29, pp. 1368–1378, Dec. 2008.
[37] D. P. R. La Campisi, B. Vegso, P. Cserti, G. Kozmann, and F. Babiloni, "Human brain distinctiveness based on EEG spectral coherence connectivity," *IEEE Trans. Biomed. Eng.*, vol. 61, no. 9, pp. 2406–2412, Sep. 2014.
[38] S. Yang and F. Deravi, "On the usability of electroencephalographic signals for biometric recognition: A survey," *IEEE Trans. Human-Mach. Syst.*, vol. 47, no. 6, pp. 958–969, Dec. 2017.
[39] R. Jenke, A. Peer, and M. Buss, "Feature extraction and selection for emotion recognition from EEG," *IEEE Trans. Affect. Comput.*, vol. 5, no. 3, pp. 327–339, Jul. 2014.
[40] S. Jirayucharoensak, S. Pan-Ngum, and P. Israsena, "EEG-based emotion recognition using deep learning network with principal component based covariate shift adaptation," *Sci. World J.*, vol. 2014, Sep. 2014, Art. no. 627892.
[41] J. L. L. Marcano, M. A. Bell, and A. A. L. Beex, "EEG channel selection for AR model based ADHD classification," in *Proc. IEEE Signal Process. Med. Biol. Symp. (SPMB)*, Dec. 2017, pp. 1–6.
[42] W.-L. Zheng and B.-L. Lu, "Investigating critical frequency bands and channels for EEG-based emotion recognition with deep neural networks," *IEEE Trans. Auton. Mental Develop.*, vol. 7, no. 3, pp. 162–175, Sep. 2015.
[43] N. Zhuang, Y. Zeng, K. Yang, C. Zhang, L. Tong, and B. Yan, "Investigating patterns for self-induced emotion recognition from EEG signals," *Sensors*, vol. 18, no. 3, p. 841, 2018.
[44] N. Zhuang, Y. Zeng, L. Tong, C. Zhang, H. Zhang, and B. Yan, "Emotion recognition from EEG signals using multidimensional information in EMD domain," *BioMed Res. Int.*, vol. 2017, Aug. 2017, Art. no. 8317357.
[45] C. Neuper and G. Pfurtscheller, "Evidence for distinct beta resonance frequencies in human EEG related to specific sensorimotor cortical areas," *Clin. Neurophysiol.*, vol. 112, pp. 2084–2097, Nov. 2001.
[46] M. Carrasco-Robles and M. Delgado-Restituto, "Mixed-signal energy feature extractor of EEG frequency bands," in *Proc. IEEE 5th Latin Amer. Symp. Circuits Syst.*, Feb. 2014, pp. 1–4.
[47] J. Yang, C. Qi, Y. Li, and J. Li, "Face recognition using extended generalized Rayleigh quotient," in *Proc. IEEE Int. Conf. Multimedia Expo*, Jul. 2017, pp. 187–192.
[48] T.-F. Wu, C.-J. Lin, and R. C. Weng, "Probability estimates for multi-class classification by pairwise coupling," *J. Mach. Learn. Res.*, vol. 5, pp. 975–1005, Dec. 2004.
[49] S. S. Poorna, P. M. V. D. S. Baba, G. L. Ramya, P. Poreddy, L. S. Aashritha, G. J. Nair, and S. Renjith, "Classification of EEG based control using ANN and KNN—A comparison," in *Proc. IEEE Int. Conf. Comput. Intell. Comput. Res.*, Dec. 2016, pp. 1–6.
[50] J. Yadav, "Classification of human emotions from EEG signals using SVM and LDA classifiers," in *Proc. Int. Conf. Signal Process. Integr. Netw.*, Feb. 2015, pp. 180–185.
[51] Y. Velchev, S. Radeva, S. Sokolov, and D. Radev, "Automated estimation of human emotion from EEG using statistical features and SVM," in *Proc. Digit. Media Ind. Academic Forum*, Jul. 2016, pp. 40–42.
[52] Z. Mu, J. Hu, and J. Min, "EEG-based person authentication using a fuzzy entropy-related approach with two electrodes," *Entropy*, vol. 18, no. 12, p. 432, 2016.

RONGKAI ZHANG received the B.S. degree from PLA Strategy Support Force Information Engineering University, Zhengzhou, China, in 2018. He is currently pursuing the M.S. degree with the China National Digital Switching System Engineering and Technological Research Center. His research interests include brain–computer interaction, cognitive neuroscience, and deep learning.

BIN YAN received the B.S. and M.S. degrees from PLA Strategy Support Force Information Engineering University, Zhengzhou, China, in 1999 and 2002, respectively, and the Ph.D. degree in physical science from the Chinese Academy of Sciences, Beijing, China, in 2005. He has been a Professor with the China National Digital Switching System Engineering and Technological Research Center, since 2015. His research interests include artificial intelligence, cognitive neuroscience, and CT image reconstruction.

LI TONG received the B.S., M.S., and Ph.D. degrees from PLA Strategy Support Force Information Engineering University, Zhengzhou, China, in 1999, 2002, and 2007, respectively. She has been an Associate Professor with the China National Digital Switching System Engineering and Technological Research Center, since 2015. Her research interests include cognitive neuroscience, deep learning, and artificial intelligence.

JUN SHU received the master's degree in measurement technology and instrumentation from Zhengzhou University, in 2008. She was cocultivated with the Institute of High Energy Physics, Chinese Academy of Sciences, from 2006 to 2008, mainly engaged in PET-related research work. Her current research interests include intelligent information processing, brain–computer interaction, and brain cognitive direction research.

XIAOXIAO SONG received the M.S. degree from PLA Strategy Support Force Information Engineering University, Zhengzhou, China, in 2007. She has been an Intermediate Engineer. She is currently with the Henan Information Center. Her research interests include the certification of RA digital certificate and e-government.

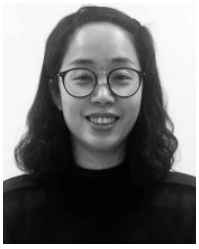

YING ZENG received the B.S., M.S., and Ph.D. degrees from PLA Strategy Support Force Information Engineering University, Zhengzhou, China, in 2004, 2007, and 2011, respectively. She is currently pursuing the Ph.D. degree with the University of Electronic Science and Technology of China, Chengdu. She has been a Lecturer with the China National Digital Switching System Engineering and Technological Research Center, since 2011. Her research interests include machine learning and cognitive neuroscience.